Journal of Molecular Structure 1131 (2017) 181–189

Contents lists available at ScienceDirect

Journal of Molecular Structure

journal homepage: http://www.elsevier.com/locate/molstruc

Synthesis, characterization and photophysical properties of luminescent non-symmetric 4-pyridyl benzothiadiazole derivatives

Alessandra Pazini [a], Luis Maqueira [b], Rafael Stieler [a], Ricardo Q. Aucélio [b], Jones Limberger [a, b, *]

[a] Laboratory of Molecular Catalysis, Institute of Chemistry – UFRGS, Av. Bento Gonçalves 9500, 91501-970, CP 15003, Porto Alegre, RS, Brazil
[b] Chemistry Department, Pontifical Catholic University of Rio de Janeiro, Rua Marquês de São Vicente, 225, Gávea, 22451-900, Rio de Janeiro, RJ, Brazil

ARTICLE INFO

Article history:
Received 29 September 2016
Received in revised form
17 November 2016
Accepted 17 November 2016
Available online 18 November 2016

Keywords:
Benzothiadiazole
Fluorescence
Cross-coupling reaction
Optical probe

ABSTRACT

Two nonsymmetrical π-extended 2,1,3-benzothiadiazoles (BTDs) bearing a 4-pyridyl moiety (**BTD-4pyr** and **BTD-Et4pyr)** were synthesized by sequential cross coupling reactions. The structural difference between the two dyes is the presence of a triple bond between the BTD core and the 4-pyridyl moiety in **BTD-Et4pyr**. The compounds architecture is similar to previously described selective mitochondrial biomarkers. Both compounds exhibit large Stokes shifts (93–137 nm), high fluorescence quantum yields and linear fluorescence response in the nanomolar range. The existence of the triple bond decreased in about 35% the fluorescence measured from **BTD-Et4pyr** in respect to **BTD-4pyr**. Solid-state fluorescence of the dyes were measured, producing considerable smaller Stokes shifts than the ones observed in solutions (74 nm for **BTD-4pyr** and 66 nm for **BTD-Et4pyr**). X-ray crystallography analysis of **BTD-4pyr** indicated a quinoid character for the BTD ring and a nonplanar relation between the BTD core and the aryl/heteroaryl groups. DFT calculations pointed out that the LUMO electron density is concentrated over the BTD core. In relation to HOMO, the electron density **is** distributed mainly at the methoxyphenyl group, in the hydrocarbon fraction of the BTD core and in ethynyl group for **BTD-Et4pyr**.

1. Introduction

Many efforts have been made in the design and synthesis of new π-conjugated molecules with luminescent properties. This search is stimulated by the large number of application of these compounds in different areas of light technology, including: OLEDs constituents [1,2]; luminescent probes for biological [3,4] and analytical chemistry [5–7]; organic sensitizers for solar cells [8], among others. In this context, 2,1,3-benzothiadiazole (BTD) derivatives with π-extended conjugation surge as privileged compounds for these applications, thanks to some relevant features, including: large Stokes shifts, BTD's strong electron withdrawing ability (which facilitates intramolecular charge transfer stabilizing processes), relatively high reduction potential and electron affinity [9].

Concerning the design of novel fluorescent probes, it is a matter of interest for both analytical chemistry and chemical biology. In the analytical point of view, the development of selective and sensitive dyes increases the range of options to perform tagging, derivatization and indirect probing for quantitative determinations. With respect to chemical biology, depending on the structure, the dyes can be used as bioprobes, capable to selective label cellular structures/macromolecules, as well as allow the study of dynamic cellular processes [3,4]. In this way, some π-extended benzothiadiazole (BTD) derivatives have emerged in last years as privileged scaffolds for selective staining organelles and cellular components. Representative examples of BTD-based bioprobes are displayed in Fig. 1.

The green emitters **1a** and **1b** selectively tagged mitochondria in three different cell lines. These compounds were designed to display two intramolecular H-bonds, which are responsible to keep the planarity e allow a putative ESIPT (excited state intramolecular proton transfer) as excited state stabilizing process [10]. The distribution of the fluorescent BTD-based glycoligand **2** was **s**tudied in living and artificial cell system. The compound is able to access the inner compartment passively and accumulates specifically in membranes [11]. The compound **3a** was produced as a probe for

* Corresponding author. Chemistry Department, Pontifical Catholic University of Rio de Janeiro, Rua Marquês de São Vicente, 225, Gávea, 22451-900, Rio de Janeiro, RJ, Brazil.
E-mail address: limberger@puc-rio.br (J. Limberger).

http://dx.doi.org/10.1016/j.molstruc.2016.11.050
0022-2860/

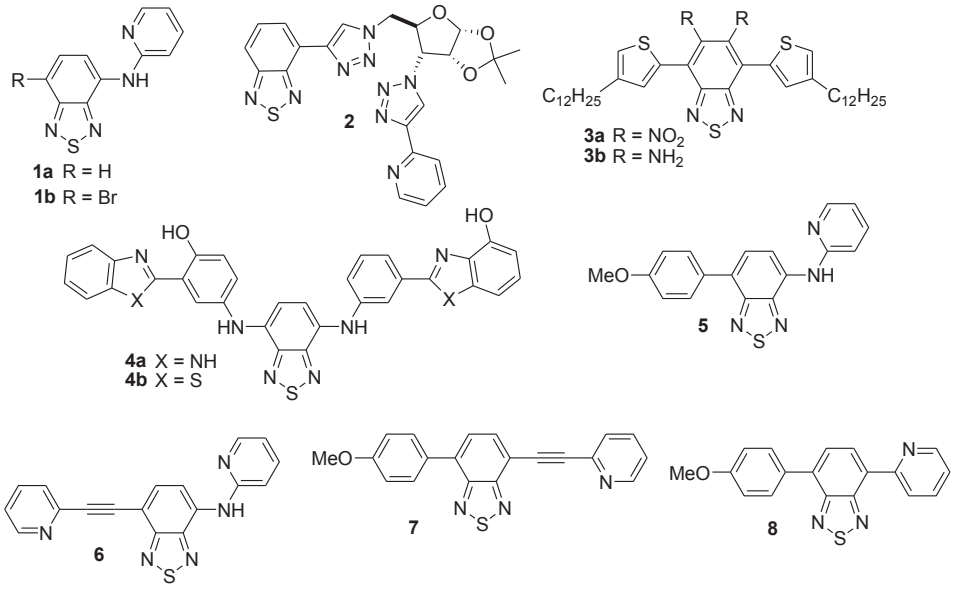

Fig. 1. Representative bioprobes based on BTD core.

hypoxic tumor cells. This NO_2-BTD derivative is nonfluorescent, however, when it was added to culture of MG63 cancer cells in hypoxic conditions, a strong red fluorescence was observed. This emission is due to the reduction of **3a** to its fluorescent NH_2-derivative **3b**. Moreover, it was determined that the presence of **3a** in cells stimulates the expression of the nitroredutase, which could improve the conversion of **3a** to **3b** [12]. The symmetric BTD derivatives **4** enable high quality images and selective staining for nuclear dsDNA in human stem cells. The compounds exhibited large stoke shifts and high stability, representing an interesting alternative to the commercial imaging probes [13]. The compounds **5** and **6** were evaluated as mitochondrial marker in cancer cells [14]. The results were not satisfactory, however it was observed that the presence of the donator group 4-methoxyphenyl in **5** was capable to increase the emission intensity and, the presence of the ethynylpyridyl group of **6** slightly enhanced the mitochondrial selectivity. Bearing these results in mind, authors synthesized the bioprobe **7**, which possess both 4-methoxyphenyl and ethynylpyridyl groups. This compound proved to be a remarkable mitochondrial dye for bioimaging experiments, allowing organelle imaging and revealing the mitochondrial dynamics during the whole cell division cycle. Another efficient and selective bioprobe for mitochondrial staining is **8** [15]. This compound structurally resembles **7**, however, lacking the triple bond spacer. Similarly to observed for **7**, the 4-methoxyphenyl group is responsible for the increasing of the fluorescence intensity whereas the 2-pyridyl group is related to organelle selection.

Taking into account the outstanding results observed for mitochondrial selection observed for **7** and **8**, this work describes the synthesis and the photophysycal characteristics, in solution and in solid phase, of the fluorescent compounds **BTD-4pyr** and **BTD-Et4pyr.** These dyes were designed considering the structural features that ensured intense emission (4-methoxyphenyl group) and selectivity (pyridyl group) to the previously described BTD-based bioprobes **7** and **8**. The compounds were obtained with good yields through sequential cross-coupling reactions, display large Stokes shifts, high fluorescence quantum yields and linear fluorescence response in the nanomolar range. Moreover, the dyes exhibit absorption/emission spectra and HOMO/LUMO electronic maps very similar to previous reported dyes.

2. Experimental

2.1. Material and instruments

All solvents (acetonitrile, methanol, acetone, ethyl acetate, tetrahydrofuran, propan-2-ol, dichloromethane, toluene, pentane and diethyl ether) were of analytical grade and purchased from Merck (Germany). Fluorescein sodium salt was form Fluka, Gemany, and NaOH was from Merck. The monoarylated intermediate **3** was synthesized using procedures described in literature [16]. Cesium fluoride (CsF) and potassium carbonate (K_2CO_3) were dried under vacuum, at 100 °C during 1 h before the use. Arilboronic acid/ester were obtained from Sigma-Aldrich and used as received. All cross-coupling reactions were performed under argon atmosphere. Toluene, tetrahydrofuran and dioxane were distillated under sodium/benzophenone before the use in reactions.

UV–vis absorption spectra were acquired on a Cary 50 single beam spectrophotometer using scan velocity of 1200 nm min^{-1}, spectral bandpass of 10 nm and 1 cm path length quartz cuvettes (two optically clear faces). Photoluminescence spectra and steady state photoluminescence measurements were performed on a PerkinElmer model LS 45 luminescence spectrophotometer with 10 nm excitation and emission spectral bandpass. Scanning was made at 1500 nm min^{-1} with solutions placed in 1 cm optical pathlength quartz cuvettes (four optically clear faces). Photoluminescence lifetimes were obtained from decay measurements using a Horiba-Jobin Ivon-IBH time correlated single photon counting fluorimeter with a 330 nm nanoLED source (N-16, 1.0 ns nominal pulse duration at 1 MHz repetition rate). Computer programs supplied by the manufacturer were employed to process the time resolved data. Nuclear resonance magnetic spectra were recorded in a Bruker (Germany) model Avance III HD 400 MHZ spectrometer. Electron spray ionization high-resolution mass spectrometric (ESI-(+) HRMS) analyses were performed on a Q-TOF (Micromass) mass spectrometer (Waters, USA) with the compounds dissolved in a 10% solution of formic acid in acetonitrile. A Bruker D8 VENTURE diffractometer outfitted with a PHOTON 100 area detector and a graphite monochromator (Mo-Kα, $\lambda = 0.71{,}073$ Å) was used to collect the X-ray data for the structural analysis of **BTD-4pyr**.

2.2. Synthesis of the BTD-derivatives

4-(4-methoxyphenyl)-7-(pyridin-4-yl)benzo[c] [1,2,5]thiadiazole **(BTD-4pyr)**: An oven-dried resealable Schlenk flask was evacuated, back-filled with argon and charged with 4-bromo-7-(4-methoxyphenyl)benzo[c] [1,2,5]thiadiazole **11** (1.0 mmol, 320 mg), $Pd(PPh_3)_4$ (0.01 mmol, 11.6 mg), 4-Pyridinylboronic acid MIDA ester (1.05 mmol, 246 mg), aqueous 1 mol L^{-1} K_2CO_3 solution (2,0 mL, 2.0 mmol) and toluene (4 mL). The reaction was stirred at 110 °C for 20 h, then allowed to cool-down to room temperature. The mixture was filtered, the solid was washed with toluene (2 × 5 mL) and the solution was concentrated under reduced pressure. The crude material was then purified by column chromatography on silica gel using hexane/ethyl acetate (10:1), providing 157 mg (49% yield) of the **BTD-4pyr** as a yellow solid. Melting point: 203 °C (decomp). ^{1}H NMR (400 MHz, $CDCl_3$) δ (ppm) 8.82 (d, J = 5.6 Hz, 2H), 8.36 (d, J = 5.6 Hz, 2H), 8.04 (d, J = 7.4 Hz, 1H), 7.99 (d, J = 8.6 Hz, 2H), 7.85 (d, J = 7.4 Hz, 1H), 7.12 (d, J = 8.6 Hz, 2H), 3.93 (s, 3H). ^{13}C NMR (100 MHz, $CDCl_3$) δ 160.15, 154.14, 153.52, 150.15, 144.71, 134.80, 130.55, 129.40, 129.36, 128.89, 126.94, 123.48, 114.18, 77.32, 77.00, 76.68, 55.41. HRMS (m/z) for $C_{18}H_{14}N_3OS$ ($M + H^+$): calculated: 320.0858. Obtained: 320.0844.

4-(4-methoxyphenyl)-7-(2-(pyridin-4-yl)ethynyl)benzo[c] [1,2,5]thiadiazole **(BTD-Et4pyr)**: An oven-dried resealable Schlenk flask was evacuated, back-filled with argon and charged with 4-bromo-7-(4-methoxyphenyl)benzo[c] [1,2,5]thiadiazole **11** (1.0 mmol, 320 mg), $PdCl_2(PPh_3)_2$ (0.01 mmol, 7.0 mg), CuI (0.02 mmol, 3.8 mg), 4-ethynylpyridyne (1.10 mmol, 113 mg), triethylamine (250 μL) and THF (4 mL). The reaction was stirred at 80 °C for 18 h, then allowed to cool-own to room temperature. The mixture was filtered, the solid was washed with THF (2 × 5 mL) and the solution was concentrated under reduced pressure. The crude material was then purified by column chromatography on silica gel using hexane/ethyl acetate (8:1) and providing 261 mg (76% yield) of the **BTD-4pyr** as a yellow solid. Melting point: 184 °C. ^{1}H NMR (400 MHz, CDCl3) δ (ppm) 8.66 (d, J = 6.0 Hz, 2H), 7.95 (d, J = 8.8 Hz, 2H), 7.92 (d, J = 7.4 Hz, 1H), 7.69 (d, J = 7.4 Hz, 1H), 7.58 (d, J = 6.0 Hz, 2H), 7.08 (d, J = 8.8 Hz, 2H), 3.90 (s, 3H). ^{13}C NMR (100 MHz, $CDCl_3$) δ (ppm) 160.3, 155.1, 153.2, 148.7, 135.7, 134.1, 132.2, 130.6, 129.1, 126.5, 126.0, 114.2, 113.5, 92.1, 91.0, 55.4. HRMS (m/Z) for $C_{20}H_{14}N_3OS$ ($M + H^+$): calculated: 344.0858. Obtained: 344.0871.

2.3. X-ray structural determination

A combination of ϕ and ω scans was carried out to obtain at least a unique data set. The crystal structure was solved using direct methods in the SHELXS program [17]. The final structure was refined using SHELXL [17], where the remaining atoms were located from difference Fourier synthesis. Anisotropic displacement parameters were applied to all non-hydrogen atoms, followed by full-matrix least-squares refinement based on F^2. All hydrogen atoms were placed in ideal positions and refined as riding atoms with relative isotropic displacement parameters. The crystallographic data and structure refinement parameters are provided in Table 1.

2.4. Theoretical calculation software

The structural parameters were estimated using the 6−31G** basis set [18]. Calculations were carried out by the density functional theory (DFT) method with the Gaussian03 program package [19]. The commonly used B3LYP (Becke, three-parameter, Lee−Yang−Parr) exchange-correlation functional approach [20] was employed as indicated for the study of other organic systems [21].

Table 1
Crystallographic data and structure refinement parameters for BTD-4pyr.

Molecular formula	$C_{18}H_{13}N_3OS$
Fw [g mol^{-1}]	319.37
T [K]	100 (2)
Crystal system	Triclinic
Space group	$P(-1)$
a [Å]	9.4071 (5)
b [Å]	9.8787(5)
c [Å]	10.0943 (6)
α [°]	110.942 (2)
β [°]	116.571 (2)
γ [°]	98.340 (3)
V [$Å^3$]	729.49 (7)
Z	2
$\rho_{calcd.}$ [g cm^{-3}]	1.454
μ [mm^{-1}]	0.230
F (000)	332
Crystal size [mm]	0.26 × 0.24× 0.07
θ range [°]	2.808 to 26.505
Limiting indices (h, k, l)	$-11 \le h \le 11$ $-12 \le k \le 12$ $-12 \le l \le 12$
Reflections collected	18,139
Reflections unique [R_{int}]	3013 [0.0404]
Completeness to θ_{max} [%]	99.8
Data/restraints/param.	3013/0/208
Absorption correction	Gaussian
Min. and max. transmission	0.95,847 and 0.98,969
R_1 [$I > 2\sigma(I)$][a]	0.0350
wR_2 [$I > 2\sigma(I)$][a]	0.0851
R_1 (all data)[a]	0.0470
wR_2 (all data)[a]	0.0921
S on F^2[a]	1.044
Largest diff. peak and hole (e.$Å^{-3}$)	0.455 and −0.266

[a] As defined by the SHELXL program [17].

2.5. Solutions

The solutions of the dyes, used for the solvent effect studies, were in the concentration of 25 μmol L^{-1}. Fluorescein sodium salt solution ($3.0 \times 10^{-7} - 1.1 \times 10^{-6}$ mol L^{-1}) was employed to estimate fluorescence quantum yields. This solution was prepared in NaOH aqueous solution (0.1 mol L^{-1}) in order to get a standard solution with fluorescence quantum efficiency (Φ_f) of 0.93, as indicated by Sjöback et al. [22]. Experiments in solid substrate were made by placing 150 μL of the dyes solutions on the center of a circular Nylon substrate (10 mm diameter) letting it in a desiccator until total evaporation of the solvent. Lifetime measurements were made using 10 μmol L^{-1} dyes solutions (dissolved in ethyl acetate).

3. Results and discussion

The proposed strategy to obtain the target 4-pyrydil-BTD dyes (Scheme 1) begun with the Suzuki cross-coupling reaction between the 4,7-dibromo-2,1,3-benzothiadiazole **9** and 4-methoxyphenylboronic acid. This reaction was performed using conditions described in literature [16] (N,C,P-palladacycle **10**,CsF, dioxane 130 °C) providing the monoarylated intermediate **11** (81% yield in 24 h). In order to obtain the luminescent compound **BTD-4pyr**, the monobrominated intermediate was reacted with the 4-pyridylboronic acid MIDA ester **12**, using another Suzuki protocol, with a system composed by $Pd(PPh_3)_4$, aqueous K_2CO_3 and toluene. This reaction afforded **BTD-4pyr** with 49% yield and 40% overall yield.

For the synthesis of the ethynyl-containing dye **BTD-Et4pyr**, the monobrominated intermediate **11** was reacted in a Sonogashira protocol with **13** under classical conditions ($PdCl_2(PPh_3)_2$, CuI, NEt_3 in THF). This reaction produced the desired product with 76% yield

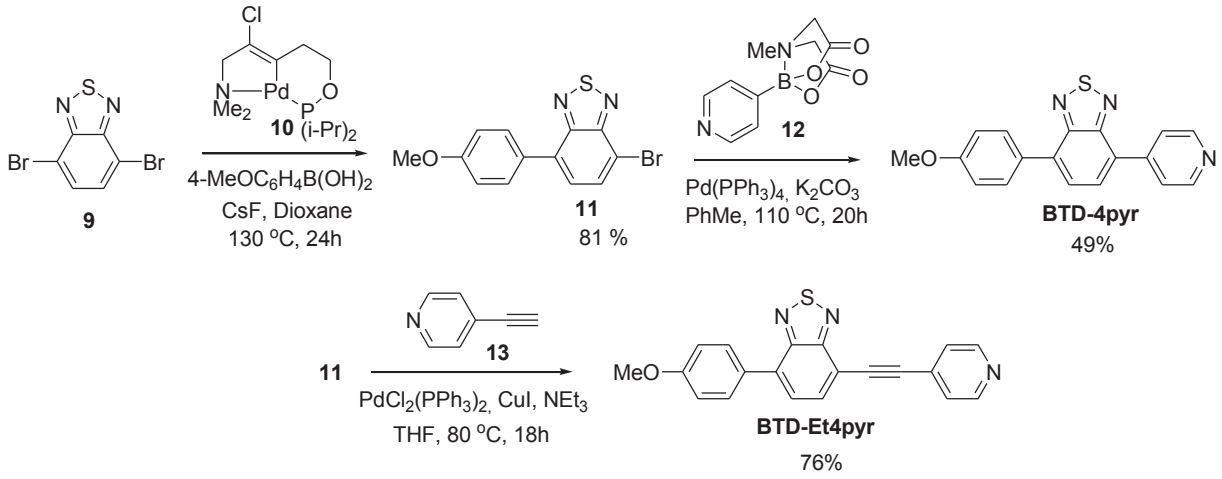

Scheme 1. Synthesis of the BTD derivatives BTD-4pyr and BTD-Et4pyr.

and overall yield of 62%.

An expansion of the aromatic region of the ^{1}H NMR of the dyes is depicted in Fig. 2. For both compounds, all aromatic/hetero-aromatic hydrogens can be observed as doublets, and the $^{3}J_{H-H}$ coupling can be easily calculated (the *J* values are described in Experimental Section). The chemical shifts of 4-methoxyaryl hydrogens H1/H1' and H2/H2' are very similar for both **BTD-4pyr** and **BTD-Et4pyr** respectively appearing around 7.1 ppm and 8.0 ppm. The insertion of ethynyl spacer between the BTD core and the 4-pyridyl group shifts upfield both BTD core hydrogens H'$_{BTD}$ in comparison with H$_{BTD}$. The triple bond spacer also affects the chemical shift of the hydrogens H3 (8.36 ppm) and H4 (8.81 ppm) in relation to H3' (7.58 p.m.) and H4' (8.66 ppm). In relation to ^{13}C NMR, the dyes spectra are similar (see Supplementary Material), the major difference is the triple bond carbons of **BTD-Et4pyr**, observed at 91.0 and 92.1 ppm.

Single crystals of **BTD4-pyr** suitable for X-ray diffraction studies were grown at room temperature from a concentrated solution of toluene. The molecular structure of the compound is shown in Fig. 3. The main crystallographic data and structure refinement parameters are reported in Table 1. Selected bond lengths are listed in Table 2. The solid-state structure of **BTD4-pyr** reveals a nonplanar molecule, with the aryl/pyridyl rings twisting each other due to the steric hindrance between the hydrogen atoms. The average dihedral angles between the pyridyl and BTD ring is 35.6(2)°. This torsion angle is similar to observed for the solid structures of 4,7-dipyridylbenzothiadiazole (36.8°) [23]. The torsion angle between the methoxyaryl ring and BTD core of the dye **BTD4-pyr** is 46.3(2)°, about 15° higher than the angles observed for the bioprobe **7** [24]. The inspection of the bond distances in the BTD skeleton suggest a quinoid character for the BTD ring [25,26] since considerable shortenings of the C8–C9, C10–C11, bonds are observed (Table 2). The quinoid form is found in many dyes and can be considered a powerful chromophore that produce intensely colored compounds [9]. The packing structure of **BTD4-pyr** is shown in Fig. 2B. Although the stacking structure is formed, the interactions between the molecules seems to be weak considering the molecular plane distances. The distance between the planes of the BTD rings is 3.33 Å. No short S···N or S···S contacts are observed in the crystal structures of the compound.

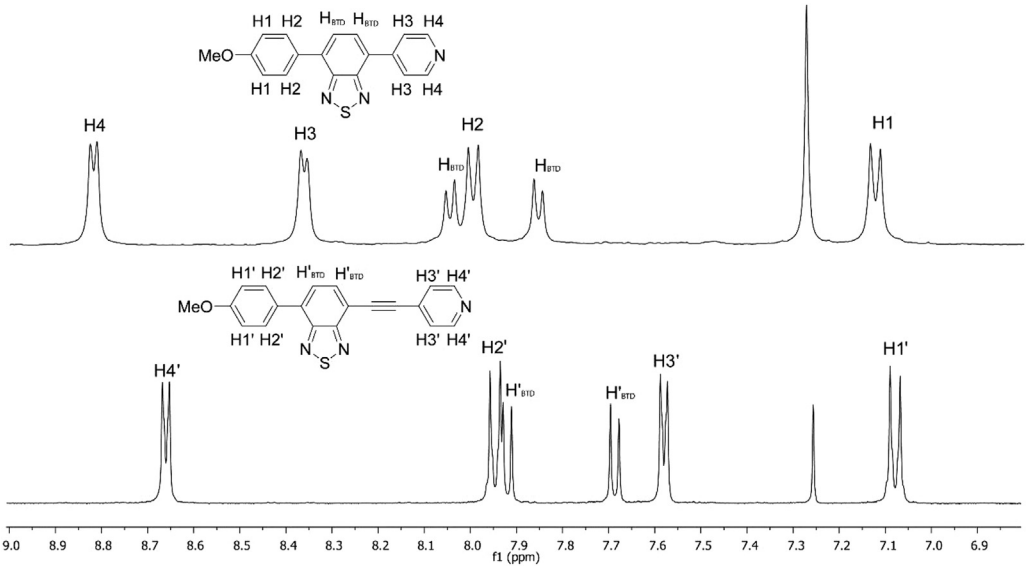

Fig. 2. Expansion of aromatic region of ^{1}H NMR spectra (400 MHz, $CDCl_3$) for **BTD-4pyr** and **BTD-Et-4pyr**.

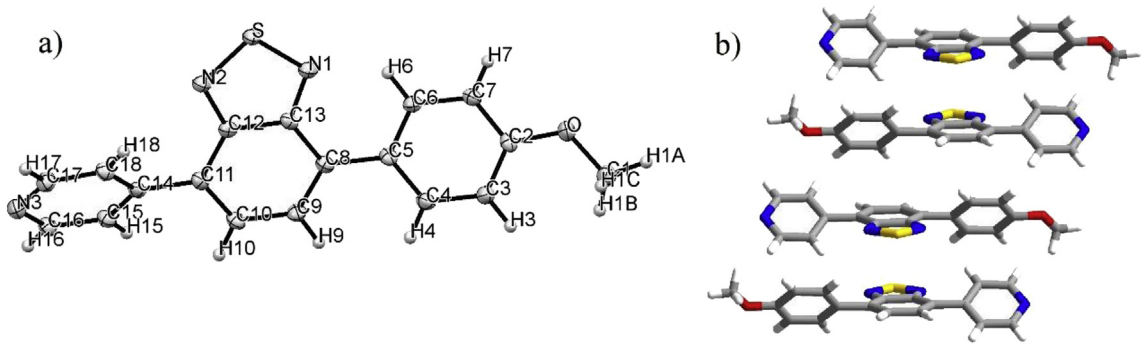

Fig. 3. a) Molecular structure of the dye **BTD4-pyr**. The ellipsoids are draw with 50% probability level. b) Packing structure of **BTD4-pyr**.

Table 2
Selected bond lengths (Å) for **BTD4-pyr**.

Bond	Bond lenght (Å)	Bond	Bond lenght (Å)
C (8)–C (9)	1.371 (2)	S–N (1)	1.6102 (14)
C (9)–C (10)	1.420 (2)	S–N (2)	1.6141 (14)
C (10)–C (11)	1.370 (2)	N (1)–C (13)	1.351 (2)
C (11)–C (12)	1.435 (2)	N (2)–C (12)	1.348 (2)
C (12)–C (13)	1.434 (2)		
C (13)–C (8)	1.431 (2)		

The UV–vis absorption spectra of the dyes were recorded at room temperature either in chloroform (Fig. 4a) or in ethyl acetate (Fig. 4b). In Fig. 4a, two strong absorption bands can be observed for both compounds. The bands centered at 321 and 311 nm are related to π-π* [18,27] transitions whereas the absorptions observed at 417 and 418 nm are attributed to intramolecular charge transfer (ICT) [18,27]. In ethyl acetate **BTD-4pyr** and **BTD-Et4pyr** presented spectral maximum at 390 and 406 nm, respectively, with FWHM of about 70 nm. The maximum of absorption observed for **BTD-4pyr** is slightly more energetic than observed in literature for the bioprobe **8** [15], whereas the **BTD-Et4pyr** absorption is observed in similar energies than **7** and its 3-pyrydyl analog [14,28]. Estimated molar absorptivities in ethyl acetate (ε_{390} and ε_{406}) were 18,300 L mol^{-1} cm^{-1} (log ε = 4.26) for **BTD-4pyr** and 9290 L mol^{-1} cm^{-1} (log ε = 3.97) for **BTD-Et4pyr**. Additionally, the calculated optical band gaps [29,30] (E_{gap}^{opt}) were 2.76 eV for **BTD-4pyr** and 2.68 eV for **BTD-Et4pyr**, which are in the appropriate range to be used in organic-light emitting diodes (between 1.5 and 5.5 eV) [9,31].

Fluorescence from the dyes were determined in several solvents and the results are depicted in Fig. 5 and in Table 3. Both compounds showed large Stokes shifts, ranging from 100 to 137 nm for **BTD-4pyr** and from 93 to 132 nm for **BTD-Et4pyr**, which is characteristic of π-extended benzothiadiazoles [9,32]. These large $\Delta\lambda_{max}$ values indicate the high stability of the excited state and a very efficient intramolecular charge transfer (ICT) in the excited state, between the methoxyphenyl group (donor) and the BTD ring (acceptor). It is important to mention that this type of donor-aceptor relation between these groups is considered essential for the high sensitivity of the BTD mitochondrial markers **7** and **8** [14,15]. For most solvents, **BTD-Et4pyr** exhibited maximum emission at slightly higher wavelengths when compared to **BTD-4pyr**. This result is in agreement with DFT results (described below), since the large π-extension of the ethynyl-BTD dye decreases the energy gap between molecular excited and ground states.

Fluorescence quantum yields (Φ_f) and the singlet lifetime (τ_f) values for both compounds were estimated. **BTD-4pyr** displayed Φ_f of 0.49, about 35% larger than the one **BTD-Et4pyr** (0.32). Such a difference can be explained in terms of a more compact and rigid structure of **BTD-4pyr**, leading to less efficient non-radiative energy loss. These Φ_f values explain the relative difference in fluorescence intensities for these two compounds. The τ_f value for **BTD-4pyr** (9.1 ns) is also larger (about 20%) than the one of **BTD-Et4pyr** (7.3 ns). As described previously for symmetric BTD derivatives [32], the BTD adjacent triple bond increases the electron-transfer between BTD core and the pyridyl group, consequently decreasing lifetime of **BTD-Et4pyr**. The radiative decay rate constants (Φ_f/τ_f) are 5.4 × 10^7 s^{-1} for **BTD-4pyr** and 4.4 × 10^7 s^{-1} for

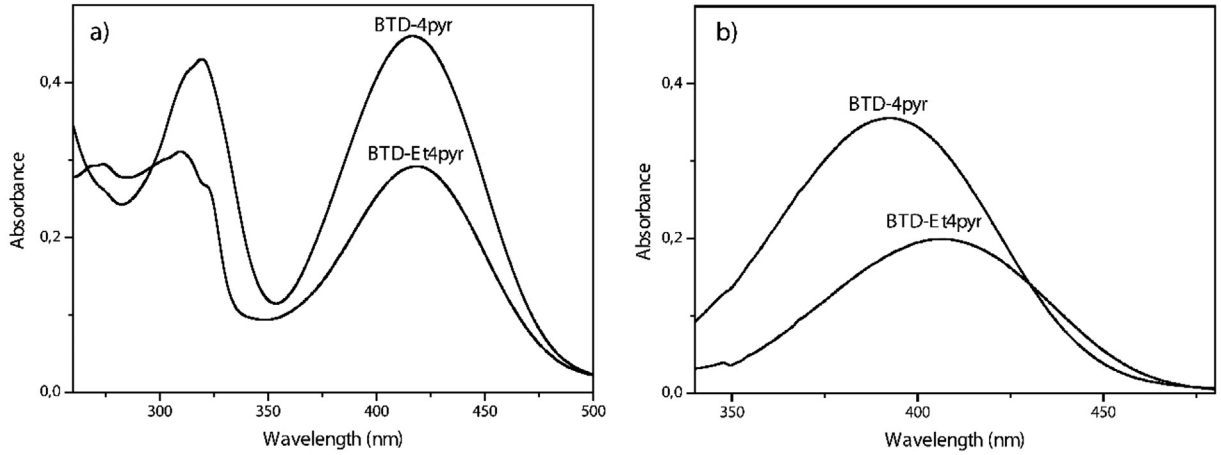

Fig. 4. Absorption spectra of **BTD-4pyr** and **BTD-Et4pyr** in chloroform (a) and in ethyl acetate (b). Concentration of dyes 25 μmol L^{-1}.

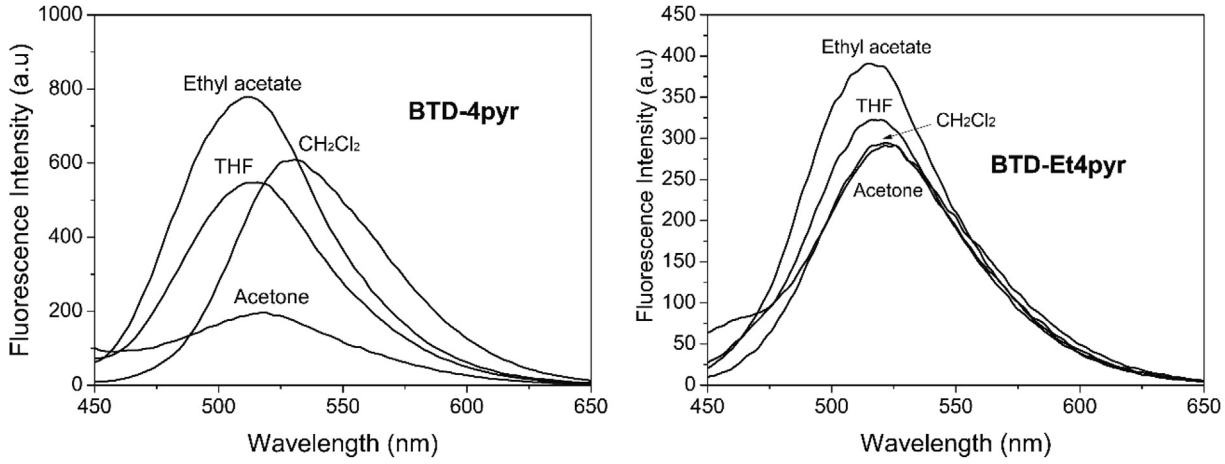

Fig. 5. Fluorescence emission spectra of **BTD-4pyr** and **BTD-Et4pyr** in different solvents. Concentration the dyes: 10 μmol L^{-1}.

Table 3
Fluorescence excitation and emission maxima and Stokes shift of **BTD-4pyr** and **BTD-Et4pyr** in different solvents.

Solvent	λ^{max}_{exc} (nm)		Polarity index	Dielectric constant	$E^N_{T(30)}$	$\Delta\lambda_{max}$	
	BTD-4pyr	**BTD-Et4pyr**				**BTD-4pyr**	**BTD-Et4pyr**
Acetonitrile	386	408	5.8	37.5	0.460	137	119
Acetone	390	408	5.1	2.07	0.355	128	113
Methanol	414	410	5.1	32.7	0.762	131	132
Ethyl Acetate	392	409	4.4	6,02	0.228	120	107
THF	396	411	4.0	7.58	0.605	118	109
Propan-2-ol	396	410	3.9	17.9	0.546	122	120
CH_2Cl_2	415	412	3.1	8.93	0.309	115	109
Toluene	400	414	2.4	2.38	0.099	100	93

BTD-Et4pyr.

The more polar the molecule, the stronger the effect of more polar solvents on the energy relaxation processes that, in turn, results in the increasing of the observed Stokes shift ($\Delta\lambda_{max}$). Taking into consideration the position of the fluorescence excitation band of the dyes (in terms λ_{exc}), it cannot be seen a clear direction for the solvatochromism using different criteria to establish the polarity of the solvent (polarity index, dielectric constant or $E^N_{T(30)}$). However, for **BTD-4pyr** it can be clearly seen an increasing of $\Delta\lambda_{max}$ as the polarity index increases, but this is not so clear for **BTD-Et4pyr** (Table 3). In contrast, for **BTD-Et4pyr**, a clear tendency for the increasing of $\Delta\lambda_{max}$ was observed as the $E^N_{T(30)}$ value increased. Such results are an indication of the stabilization of the luminophore excited state relative to the ground state as the solvent polarity increased and that these dyes permanent dipole moment increases upon excitation.

The Lippert-Mataga [33] plot (Fig. 6), which establish the relationship between the Stokes shift (cm^{-1}) and solvent polarity values (reported in terms of E^N_T) [34] expecting that the higher the E^N_T the wider the Stokes shift (expected order of Spectral shifts: Methanol > THF > propan-2-ol > acetonitrile > acetone > dichloromethane > ethyl acetate > toluene). An almost perfect correlation between solvent polarity and Stokes shift was found for **BTD-Et4pyr** ($R^2 > 0.80$), with only THF producing a magnitude of the spectral shift less than what was expected. The presence of the triple bond might facilitate solvation thus producing the more stable excited states in the presence of more polar solvents. For **BTD-4pyr** the correlation does not exactly obey the polarity order ($R^2 > 0.44$) but still shows higher spectral shifts for the relatively more polar solvents (exception made for THF that also produced a smaller Stokes shift than expected). In Fig. 3, it can be seen that the polarity of solvent (the effect of four solvents are shown) has a higher influence on the intensity and spectral positon of **BTD-4pyr** emission band than for **BTD-Et4pyr**.

Upon illumination by a hold-hand UV lamp, both dyes are bright emissive in the green. In order to quantify this effect, the fluorescence spectra of the compounds were obtained directly from the solid materials (onto a Nylon substrate). Broad spectra were obtained with significantly smaller Stokes shifts, in comparison with solution. For **BTD-4pyr** the $\lambda_{exc}/\lambda_{em}$ pair was 406/480 nm ($\Delta\lambda_{max} = 74$ nm) while for **BTD-Et4pyr** the $\lambda_{exc}/\lambda_{em}$ pair was 417/483 nm ($\Delta\lambda_{max} = 66$ nm) as can be seen in Fig. 7.

In order to better understand the relationship between the structure of the dyes and its electronic properties, it was performed a quantum mechanical theoretical investigation. Self-consistent density-functional calculations (DFT) were used to provide accurate description of the electronic distribution and atomic arrangements of these compounds and a qualitative estimate of their HOMO and LUMO energies. The molecular structures were optimized considering a vacuum environment, using Gaussian03 package [19].

In Fig. 8, the ground-state structure parameters of the BTDs and the contours of their HOMO and LUMO are shown. As can be seen, for both compounds, the LUMO electron density is concentrated over the BTD core. In relation to HOMO, the electron density are distributed mainly at the methoxyphenyl group (donor), in the hydrocarbon fraction of the BTD core and in ethynyl group for **BTD-Et4pyr**.The LUMO and HOMO distribution orbital corroborates the highly efficient donor-acceptor character of these dyes, with intramolecular charge transfer (ICT) between BTD core (electron acceptor group) and the methoxyphenyl (donor group). The

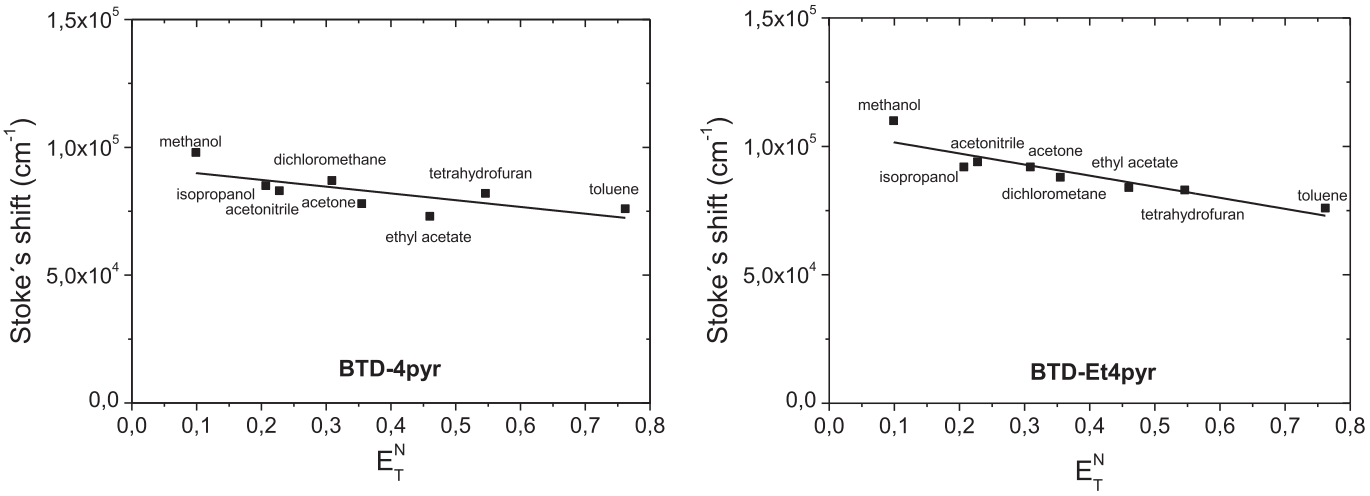

Fig. 6. Stoke's shift (cm^{-1}) of dyes in function of E_T^N values for in different solvents. BTD-4pyr (R^2>0.80), BTD-Et4pyr (R^2>0.44). Concentration of dyes: 10 μmol L^{-1}.

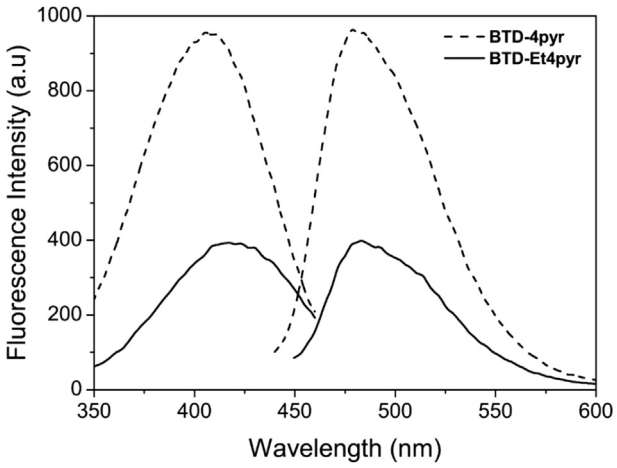

Fig. 7. Fluorescence excitation and emission spectra of the dyes in the solid state of **BTD-4pyr** and **BTD-Et4pyr**.

HOMO-LUMO band-gap energies were also calculated and the results are shown in Table 4. The obtained values were 3.15 eV for **BTD-4pyr** and 2.95 eV for **BTD-Et4pyr**. It is noteworthy that the electronic map of the fluorophores is very similar to previously described bioprobes and the band gap of the 4-pyridyl fluorophores are smaller than the observed for 2-pyridyl analogs **7** and **8** [14,15].

In terms of optimized conformation, the calculated structure of the **BTD-Et4pyr** showed a *quasi*-coplanar conformation between pyridyl ring and the BTD core, whereas the **BTD-4pyr** presented a twist of the pyridyl group. The torsion angle calculated between pyridyl groups and BTD core (35.1°) was similar to those obtained from X-ray diffraction analysis (35.6°). In general, the dihedral angles and energies values calculated are similar to others BTD-aryl and BTD-ethynylaryl derivatives already reported [14,27]. With respect to bond distances, the DFT results and X-ray diffraction of **BTD-4pyr** are in agreement, since both techniques indicated a shortening in C8–C9 and C10–C11 bonds, suggesting a quinoid character for the BTD skeleton. A similar shortening was also observed in DFT results for **BTD-Et4pyr** (Table S3 of Supplementary Material).

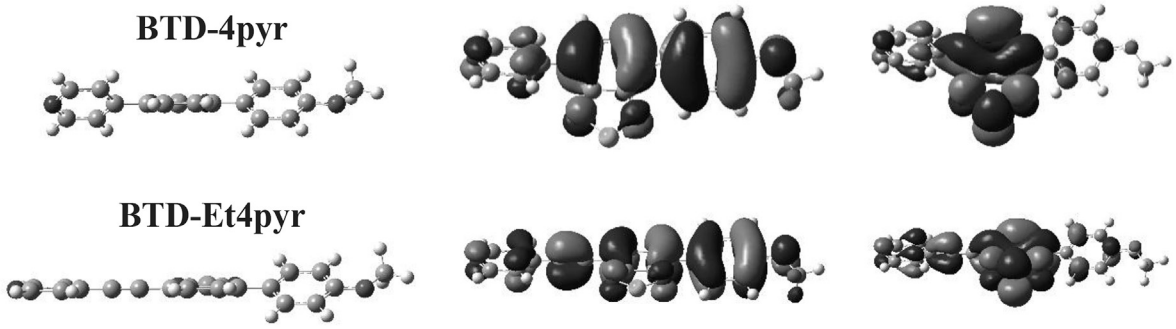

Fig. 8. Optimized structures and frontier molecular orbitals of **BTD-4pyr** and **BTD-Et4pyr**, calculated in the gas phase.

Table 4
Theoretical calculated data for BTDs synthetized at B3LYP/6-31G** in gas phase.

BTD	HOMO (eV)	LUMO (eV)	HOMO-LUMO gap (eV)	D.A (degree) (BTD/Pyridyl)	D.A (degree) (BTD/4-MeOPh)
BTD-4pyr	−5.70	−2.55	3.15	35,1	35,3
BTD-Et4pyr	−5.60	−2.65	2.95	4.9	34.0

Fluorescence response of both compounds were studied using analytical curves prepared in ethyl acetate within the nmol L^{-1} range and signal measurements made at the maximum excitation/emission wavelengths (Fig. 9). The analytical response was linear in the range covering 0.1–100 nmol L^{-1} with R^2 of 0.997 for **BTD-4pyr** and 0.999 for **BTD-Et4pyr**. The linear equation models were: $F_{\textbf{BTD-4pyr}} = (7.85 \times 10^9 \pm 1.5 \times 10^8)C_{\textbf{BTD-4pyr}} + (14.28 \pm 6.1)$ and $F_{\textbf{BTD-Et4pyr}} = (4.40 \times 10^9 \pm 1.6 \times 10^7)C_{\textbf{BTD-Et4pyr}} + (4.54 \pm 0.7)$, where F is measured fluorescence intensity and C is dye concentration. From these curves, the limits of detection were calculated (using the 3 s_{blank}/m, where s_{blank} was the standard deviation of the blank and m is the sensitivity of the analytical curve) and the values were 0.17 nmol L^{-1} for **BTD-4pyr** and 0.27 nmol L^{-1} for **BTD-Et4pyr**. These results indicates the good quality of the optical response of these dyes in potential quantitative applications as analytical probes or markers.

4. Conclusions

In summary, the work describes the two-step synthesis and the photophysical properties of two nonsymmetrical fluorescent 4-pirydyl-BTD derivatives in solid state and solution. The compounds were obtained with good yields, display wide Stokes shifts (93–137 nm), high fluorescence quantum yields and lifetimes in the ns range. Fluorescence intensity presented a linear response in function of concentration in the nanomolar range. Theoretical calculation shown that the HOMO, the electron distributions are located mainly at the methoxyphenyl group (donor), in the hydrocarbon fraction of the BTD core and in ethynyl group for **BTD-Et4pyr**. The insertion of the triple bond in fluorophe structure causes: (i) a small bathochromic shift, (ii) a considerable decrease in the fluorescence intensity, (iii) a reduction in both optical and theoretical bandgap, and (iv) spread of HOMO electronic density over the triple bond. The structural and emission properties of the 4-pirydyl dyes are very similar to its 2-pirydyl analogs, which present selective mitochondrial staining properties. Therefore the dyes studied here are potential probes to selective tag this organelle. Moreover, the calculated band gap of both dyes is in the appropriate range for its application as OLEDS. The technological use of **BTD-4pyr** and **BTD-Et4pyr** in terms of light emitters will be reported in a future work.

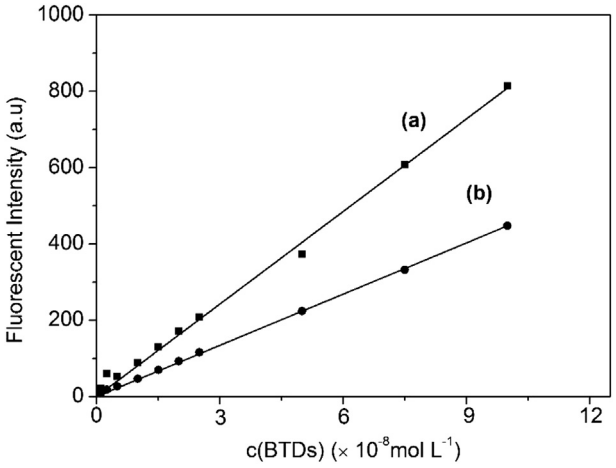

Fig. 9. Analytical curve of BTDs in ethyl acetate ($1 \times 10^{-9} - 1 \times 10^{-7}$ mol/L), excitation wavelength **BTD-4pyr** (a) (390 nm) and **BTD-Et4pyr** (b) (409 nm).

Acknowledgements

J.L. thank CNPq and VRAC-PUC-Rio for financial support. A.P. also thank CNPq for scholarship. R.Q.A. thank CNPq and FAPERJ for scholarships. We are grateful to Prof. Sonia Louro for the fluorescence lifetimes experiments and to Prof. Jairton Dupont for the use of LAMOCA facilities.

Appendix A. Supplementary data

Supplementary data related to this article can be found at http://dx.doi.org/10.1016/j.molstruc.2016.11.050.

References

[1] D. Volz, M. Wallesch, C. Fléchon, M. Danz, A. Verma, J.M. Navarro, D.M. Zink, S. Bräse, T. Baumann, Green Chemistry CRITICAL REVIEW from iridium and platinum to copper and carbon: new avenues for more sustainability in organic light-emitting diodes, Green Chem. 17 (2015) 1988–2011, http://dx.doi.org/10.1039/c4gc02195a.
[2] H. Jiang, J. Sun, J. Zhang, A review on synthesis of carbazole-based chromophores as organic light-emitting materials, Curr. Org. Chem. 16 (2012) 2014–2025, http://dx.doi.org/10.2174/138527212803251604.
[3] B.A.D. Neto, P.H.P.R. Carvalho, J.R. Correa, Benzothiadiazole derivatives as fluorescence imaging probes: beyond classical scaffolds, Acc. Chem. Res. 48 (2015) 1560–1569, http://dx.doi.org/10.1021/ar500468p.
[4] L.D. Lavis, R.T. Raines, Bright building blocks for chemical biology, ACS Chem. Biol. 9 (2014) 855–866, http://dx.doi.org/10.1021/cb500078u.
[5] M.J. Culzoni, A. Muñoz de la Peña, A. Machuca, H.C. Goicoechea, R. Babiano, Rhodamine and BODIPY chemodosimeters and chemosensors for the detection of Hg^{2+}, based on fluorescence enhancement effects, Anal. Methods 5 (2013) 30–49, http://dx.doi.org/10.1039/C2AY25769F.
[6] J. Wu, G. Lai, Z. Li, Y. Lu, T. Leng, Y. Shen, C. Wang, Novel 2,1,3-benzothiadiazole derivatives used as selective fluorescent and colorimetric sensors for fluoride ion, Dye. Pigment. 124 (2016) 268–276, http://dx.doi.org/10.1016/j.dyepig.2015.09.021.
[7] Y. Yu, C. Dong, An efficient colorimetric and fluorescent probe for the detection of fluoride ions based on a benzothiadiazole derivative, Anal. Methods 7 (2015) 9604–9608, http://dx.doi.org/10.1039/C5AY02108A.
[8] Y. Wu, W. Zhu, Organic sensitizers from D–π–A to D–A–π–A: effect of the internal electron-withdrawing units on molecular absorption, energy levels and photovoltaic performances, Chem. Soc. Rev. 42 (2013) 2039–2058, http://dx.doi.org/10.1039/C2CS35346F.
[9] B.A.D. Neto, A.A.M. Lapis, E.N. da Silva Júnior, J. Dupont, 2,1,3-Benzothiadiazole and derivatives: synthesis, properties, reactions, and applications in light technology of small molecules, Eur. J. Org. Chem. 2013 (2013) 228–255, http://dx.doi.org/10.1002/ejoc.201201161.
[10] B.A.D. Neto, P.H.P.R. Carvalho, D.C.B.D. Santos, C.C. Gatto, L.M. Ramos, N.M. de Vasconcelos, J.R. Corrêa, M.B. Costa, H.C.B. de Oliveira, R.G. Silva, Synthesis, properties and highly selective mitochondria staining with novel, stable and superior benzothiadiazole fluorescent probes, RSC Adv. 2 (2012) 1524–1532, http://dx.doi.org/10.1039/C1RA00701G.
[11] L. Garcia, M. Lazzaretti, A. Diguet, F. Mussi, F. Bisceglie, J. Xie, G. Pelosi, A. Buschini, D. Baigl, C. Policar, An intrinsically fluorescent glycoligand for direct imaging of ligand trafficking in artificial and living cell systems, New J. Chem. 37 (2013) 3030–3034, http://dx.doi.org/10.1039/c3nj00380a.
[12] Q. Jiang, Z. Zhang, J. Lu, Y. Huang, Z. Lu, Y. Tan, Q. Jiang, A novel nitro-substituted benzothiadiazole as fluorescent probe for tumor cells under hypoxic condition, Bioorg. Med. Chem. 21 (2013) 7735–7741, http://dx.doi.org/10.1016/j.bmc.2013.10.019.
[13] F.F.D. Oliveira, D.C.B.D. Santos, A.A.M. Lapis, J.R. Corrêa, A.F. Gomes, F.C. Gozzo, P.F. Moreira, V.C. de Oliveira, F.H. Quina, B.A.D. Neto, On the use of 2,1,3-benzothiadiazole derivatives as selective live cell fluorescence imaging probes, Bioorg. Med. Chem. Lett. 20 (2010) 6001–6007, http://dx.doi.org/10.1016/j.bmcl.2010.08.073.
[14] P.H.P.R. Carvalho, J.R. Correa, B.C. Guido, C.C. Gatto, H.C.B. De Oliveira, T.A. Soares, B.A.D. Neto, Designed benzothiadiazole fluorophores for selective mitochondrial imaging and dynamics, Chem. A Eur. J. 20 (2014) 15360–15374, http://dx.doi.org/10.1002/chem.201404039.
[15] B.A.D. Neto, J.R. Corrêa, P.H.P.R. Carvalho, D.C.B.D. Santos, B.C. Guido, C.C. Gatto, H.C.B. de Oliveira, M. Fasciotti, M.N. Eberlin, E.N. da Silva Jr., Selective and efficient mitochondrial staining with designed 2,1,3-benzothiadiazole derivatives as live cell fluorescence imaging probes, J. Braz. Chem. Soc. 23 (2012) 770–781, http://dx.doi.org/10.1590/S0103-50532012000400024.
[16] F.S. Mancilha, L. Barloy, F.S. Rodembusch, J. Dupont, M. Pfeffer, Cyclopalladated complexes of 4-aryl-2,1,3-benzothiadiazoles: new emitters in solution at room temperature, Dalt. Trans. 40 (2011) 10535–10544, http://dx.doi.org/10.1039/c1dt10666j.
[17] G.M. Sheldrick, A short history of SHELX, Acta Crystallogr. Sect. A 64 (2008)

112–122, http://dx.doi.org/10.1107/S0108767307043930.
[18] R. Misra, P. Gautam, Tuning of the HOMO–LUMO gap of donor-substituted symmetrical and unsymmetrical benzothiadiazoles, Org. Biomol. Chem. 12 (2014) 5448–5457, http://dx.doi.org/10.1039/c4ob00629a.
[19] M.J. Frisch, G.W. Trucks, H.B. Schlegel, G.E. Scuseria, M.A. Robb, J.R. Cheeseman, J.A. Montgomery Jr., T. Vreven, K.N. Kudin, J.C. Burant, J.M. Millam, S.S. Iyengar, J. Tomasi, V. Barone, B. Mennucci, M. Cossi, G. Scalmani, N. Rega, G.A. Petersson, H. Nakatsuji, M. Hada, M. Ehara, K. Toyota, R. Fukuda, J. Hasegawa, M. Ishida, T. Nakajima, Y. Honda, O. Kitao, H. Nakai, M. Klene, X. Li, J.E. Knox, H.P. Hratchian, J.B. Cross, V. Bakken, C. Adamo, J. Jaramillo, R. Gomperts, R.E. Stratmann, O. Yazyev, A.J. Austin, R. Cammi, C. Pomelli, J.W. Ochterski, P.Y. Ayala, K. Morokuma, G.A. Voth, P. Salvador, J.J. Dannenberg, V.G. Zakrzewski, S. Dapprich, A.D. Daniels, M.C. Strain, O. Farkas, D.K. Malick, A.D. Rabuck, K. Raghavachari, J.B. Foresman, J.V. Ortiz, Q. Cui, A.G. Baboul, S. Clifford, J. Cioslowski, B.B. Stefanov, G. Liu, A. Liashenko, P. Piskorz, I. Komaromi, R.L. Martin, D.J. Fox, T. Keith, M.A. Al-Laham, C.Y. Peng, A. Nanayakkara, M. Challacombe, P.M.W. Gill, B. Johnson, W. Chen, M.W. Wong, C. Gonzalez, J.A. Pople, Gaussian 03, Revision B.01, 2003.
[20] A.D. Becke, Density-functional thermochemistry. III. The role of exact exchange, J. Chem. Phys. 98 (1993) 5648–5652, http://dx.doi.org/10.1063/1.464913.
[21] J. Tirado-Rives, W.L. Jorgensen, Performance of B3LYP density functional methods for a large set of organic molecules, J. Chem. Theory Comput. 4 (2008) 297–306, http://dx.doi.org/10.1021/ct700248k.
[22] R. Sjöback, J. Nygren, M. Kubista, Absorption and fluorescence properties of fluorescein, Spectrochim. Acta Part A Mol. Biomol. Spectrosc. 51 (1995) L7–L21, http://dx.doi.org/10.1016/0584-8539(95)01421-P.
[23] M. Akhtaruzzaman, M. Tomura, J. Nishida, Y. Yamashita, Synthesis and characterization of novel dipyridylbenzothiadiazole and bisbenzothiadiazole derivatives, J. Org. Chem. 69 (2004) 2953–2958, http://dx.doi.org/10.1021/jo035800h.
[24] B.A.D. Neto, A.A.M. Lapis, F.S. Mancilha, E.L. Batista Jr., P.A. Netz, F. Rominger, L.A. Basso, D.S. Santos, J. Dupont, On the selective detection of duplex deoxyribonucleic acids by 2,1,3-benzothiadiazole fluorophores, Mol. Biosyst. 6 (2010) 967–975, http://dx.doi.org/10.1039/b919155k.
[25] T. Suzuki, T. Tsuji, T. Okubo, A. Okada, Y. Obana, T. Fukushima, T. Miyashi, Y. Yamashita, Preparation, structure, and amphoteric redox properties of p -Phenylenediamine-Type dyes fused with a chalcogenadiazole unit, J. Org. Chem. 66 (2001) 8954–8960, http://dx.doi.org/10.1021/jo010808h.
[26] M. Tomura, Y. Yamashita, Crystal structure of 4,7-dibromo-2,1,3-benzothiadiazole, C6H2Br2N2S, Z. Für Krist. - New Cryst. Struct. 218 (2003) 555–556, http://dx.doi.org/10.1524/ncrs.2003.218.4.555.
[27] C. Wang, M. Wu, Y. Hu, W. Wu, J. Su, J. Li, 5-Phenyl-iminostilbene based organic dyes for efficient dye-sensitized solar cells, Tetrahedron 70 (2014) 6241–6248, http://dx.doi.org/10.1016/j.tet.2014.02.074.
[28] B.A.D. Neto, A.A.M. Lapis, F.S. Mancilha, I.B. Vasconcelos, C. Thum, L.A. Basso, D.S. Santos, J. Dupont, New sensitive fluorophores for selective DNA detection, Org. Lett. 9 (2007) 4001–4004, http://dx.doi.org/10.1021/ol701708y.
[29] A.K. Agrawal, S.A. Jenekhe, Electrochemical properties and electronic structures of conjugated polyquinolines and polyanthrazolines, Chem. Mater 8 (1996) 579–589, http://dx.doi.org/10.1021/cm9504753.
[30] M.M. Alam, S.A. Jenekhe, Conducting ladder polymers: insulator-to-metal transition and evolution of electronic structure upon protonation by poly(-styrenesulfonic acid), J. Phys. Chem. B 106 (2002) 11172–11177, http://dx.doi.org/10.1021/jp021230y.
[31] R.P. Ortiz, M.C. Ruiz Delgado, J. Casado, V. Hernández, O.-K. Kim, H.Y. Woo, J.T. López Navarrete, Electronic modulation of dithienothiophene (DTT) as π-center of d-π-d chromophores on optical and redox properties: analysis by UV–Vis–NIR and raman spectroscopies combined with electrochemistry and quantum chemical DFT calculations, J. Am. Chem. Soc. 126 (2004) 13363–13376, http://dx.doi.org/10.1021/ja047058o.
[32] B.A. DaSilveira Neto, A.S. Lopes, G. Ebeling, R.S. Gonçalves, V.E.U. Costa, F.H. Quina, J. Dupont, Photophysical and electrochemical properties of π-extended molecular 2,1,3-benzothiadiazoles, Tetrahedron 61 (2005) 10975–10982, http://dx.doi.org/10.1016/j.tet.2005.08.093.
[33] D. Patra, C. Barakat, Synchronous fluorescence spectroscopic study of solvatochromic curcumin dye, Spectrochim. Acta Part A Mol. Biomol. Spectrosc. 79 (2011) 1034–1041, http://dx.doi.org/10.1016/j.saa.2011.04.016.
[34] C. Reichardt, Solvatochromic dyes as solvent polarity indicators, Chem. Rev. 94 (1994) 2319–2358, http://dx.doi.org/10.1021/cr00032a005.